

## Structural and magnetic properties of amorphous $(\text{Zr}_{65}\text{Al}_{7.5}\text{Cu}_{17.5}\text{Ni}_{10})_{100-x}\text{Fe}_x$ alloys

This article has been downloaded from IOPscience. Please scroll down to see the full text article.

1998 J. Phys.: Condens. Matter 10 L575

(<http://iopscience.iop.org/0953-8984/10/34/001>)

View [the table of contents for this issue](#), or go to the [journal homepage](#) for more

Download details:

IP Address: 171.66.16.151

The article was downloaded on 12/05/2010 at 23:27

Please note that [terms and conditions apply](#).

## LETTER TO THE EDITOR

## Structural and magnetic properties of amorphous (Zr<sub>65</sub>Al<sub>7.5</sub>Cu<sub>17.5</sub>Ni<sub>10</sub>)<sub>100-x</sub>Fe<sub>x</sub> alloys

N Mattern†§, S Roth†, G Henninger‡, H Hermann† and J Eckert†

† Institute of Solid State and Materials Research Dresden, PO Box 27 00 16, D-01171 Dresden, Germany

‡ Technical University Dresden, Institute of Materials Science, Helmholtzstrasse 7, D-01069 Dresden, Germany

Received 3 July 1998

**Abstract.** Structural and magnetic properties of rapidly quenched amorphous (Zr<sub>65</sub>Al<sub>7.5</sub>Cu<sub>17.5</sub>Ni<sub>10</sub>)<sub>100-x</sub>Fe<sub>x</sub> alloys were investigated as a function of the iron content ( $x = 0$  to 20). The observed dependence of the atomic pair correlation functions on the Fe content points to the random incorporation of the iron atoms into the amorphous structure. The magnetic behaviour is dominated by temperature independent Pauli paramagnetism in the range  $x \leq 15$ . Magnetic clusters are determined for  $x = 20$ . The appearance of these iron clusters is consistent with the observed random distribution of iron atoms in the amorphous alloy. The minimum size of an iron cluster required for the creation of a non-zero magnetic moment amounts to about 100 atoms.

Amorphous Zr<sub>65</sub>Al<sub>7.5</sub>Cu<sub>17.5</sub>Ni<sub>10</sub> can be obtained at low cooling rates enabling the preparation of bulk metallic glasses. The alloy belongs to the new class of amorphous metallic alloys [1–3] which is characterized by an extended temperature span between glass transition temperature  $T_g$  and the crystallization temperature  $T_x$ . Recently, Fe-based amorphous soft magnetic alloys with an extended supercooled liquid region have also been reported [4, 5]. Adding up to 20 at.% iron to the bulk glass forming Zr<sub>65</sub>Al<sub>7.5</sub>Cu<sub>17.5</sub>Ni<sub>10</sub> alloy is was found to maintain a still reasonable extension of the temperature range of the undercooled liquid [6] (see table 1). However,  $T_g$  and  $T_x$  change and it is of interest to study the influence of iron addition on the structural and magnetic properties of amorphous Zr<sub>65</sub>Al<sub>7.5</sub>Cu<sub>17.5</sub>Ni<sub>10</sub>.

**Table 1.** Structural parameters and thermal properties of amorphous (Zr<sub>65</sub>Al<sub>7.5</sub>Cu<sub>17.5</sub>Ni<sub>10</sub>)<sub>100-x</sub>Fe<sub>x</sub>.

	$x = 0$	$x = 5$	$x = 10$	$x = 15$	$x = 20$
$s_1$ (nm <sup>-1</sup> )	25.7	25.9	26.2	26.4	26.6
$s_2/s_1$	44.3	44.2	44.1	44.6	45.2
$r_1$ (nm)	0.308	0.301	0.297	0.293	0.290
$T_g$ (K)	637	651	669	681	693
$T_{x-max}$ (K)	744	723	732	738	743

Amorphous (Zr<sub>65</sub>Al<sub>7.5</sub>Cu<sub>17.5</sub>Ni<sub>10</sub>)<sub>100-x</sub>Fe<sub>x</sub> ( $x = 0, 5, 10, 15, 20$ ) ribbons 10 mm in width and 25  $\mu$ m in thickness were prepared by rapid quenching from the melt. X-ray diffraction

§ Corresponding author. Electronic mail: n.mattern@ifw-dresden.de.

(XRD) patterns were recorded by a Philips PW 3020 Bragg–Brentano diffractometer using Mo  $K\alpha$  radiation. The thermal behaviour was investigated by a Netzsch 404 DSC at a heating rate of 20 K  $\text{min}^{-1}$ . The magnetization was measured as a function of the external field and the temperature using a SQUID magnetometer. The temperature ranged from 1.5 K to 300 K and the field,  $\mu_0 H$ , varied between  $-5$  T and  $+5$  T.

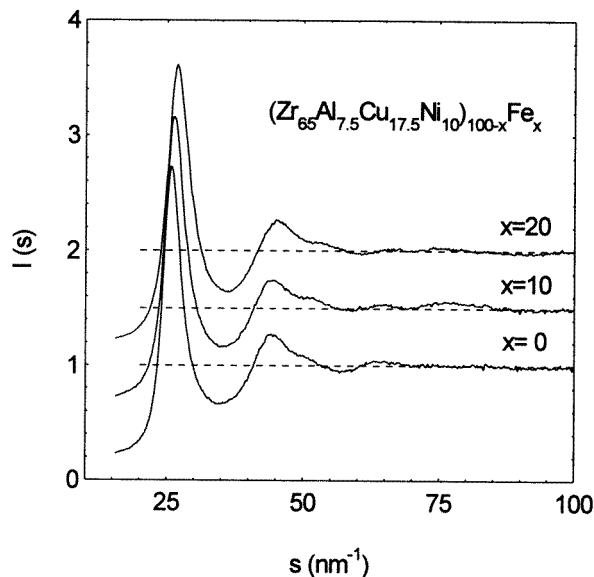


**Figure 1.** Interference functions  $I(s)$  of amorphous  $(\text{Zr}_{65}\text{Al}_{7.5}\text{Cu}_{17.5}\text{Ni}_{10})_{100-x}\text{Fe}_x$ .

Figure 1 shows the interference functions  $I(s)$  ( $s$  is the absolute value of the scattering vector  $s = 4\pi \sin \Theta / \lambda$ ) of different  $(\text{Zr}_{65}\text{Al}_{7.5}\text{Cu}_{17.5}\text{Ni}_{10})_{100-x}\text{Fe}_x$  alloys in the as-quenched state. The  $I(s)$  curves show the behaviour which is typical for a metallic glass, i.e. a shoulder appears in the second diffuse maximum. The addition of Fe leads to some changes in the interference function. The most remarkable difference is the shift of the maximum position of the first diffuse peak. The position of the first maximum is shifted to higher  $s$ -values with increasing iron content  $x$  (table 1). A linear extrapolation to  $x = 100$  (100% Fe) gives  $s_1 = 31 \text{ nm}^{-1}$ , which is similar to the value for amorphous iron or amorphous iron based alloys [7]. The continuous shift of the first diffuse maximum with iron content points to the random incorporation of the iron atoms into the amorphous structure. A decomposition into iron clusters and an iron-free amorphous phase should be indicated by a broadening or splitting of a submaximum at  $31 \text{ nm}^{-1}$ . This is not observed. From the linear shift of the first maximum in  $I(s)$  we conclude the formation of a homogeneous amorphous phase.

From the interference function  $I(s)$  the reduced atomic pair correlation function  $G(r)$  was calculated by the Fourier transform [7]

$$G(r) = 4\pi r(\rho - \rho_0) = \frac{2}{\pi} \int I(s) \sin(sr) ds \quad (1)$$

where  $\rho$  is the atomic pair density distribution function and  $\rho_0$  is the mean atomic density. Figure 2 shows the estimated  $G(r)$ -curves. All these curves exhibit a second split maximum as found to be typical for amorphous metallic alloys [7]. The positions of the maxima in  $G(r)$  decrease with increasing iron content.

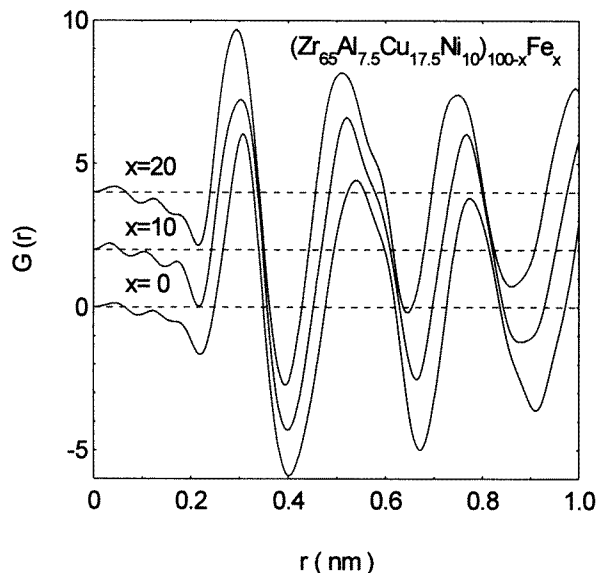


Figure 2. Pair correlation function  $G(r)$  of amorphous  $(\text{Zr}_{65}\text{Al}_{7.5}\text{Cu}_{17.5}\text{Ni}_{10})_{100-x}\text{Fe}_x$ .

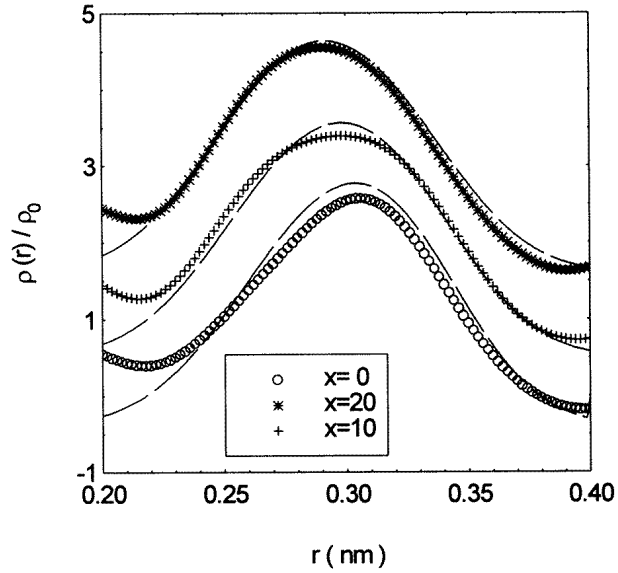
The measured interference function  $I(s)$  and the estimated  $G(r)$ -curves represent the weighted sum of the  $n(n+1)/2$  partial interference functions  $I_{ij}(s)$  in the  $n$ -component alloy [8, 9], i.e.  $I(s) = \sum_{i,j} w_{ij} I_{ij}(s)$  and  $G(r) = \sum_{i,j} w_{ij} G_{ij}(r)$ . With increasing iron content the weights  $w_{ij}$  of the individual partial functions are altered. Therefore, the visible changes in  $I(s)$  and  $G(r)$  are correlated with the variation of the iron content. The first maximum of  $G(r)$  at  $r_1$  represents a superposition of the first-neighbour distances  $r_{1,ij}$ ,

$$r_1 = \sum_{i,j} c_i f_i f_j N_{1,ij} r_{1,ij} \left( \sum_{i,j} c_i f_i f_j N_{1,ij} \right)^{-1} \quad (2)$$

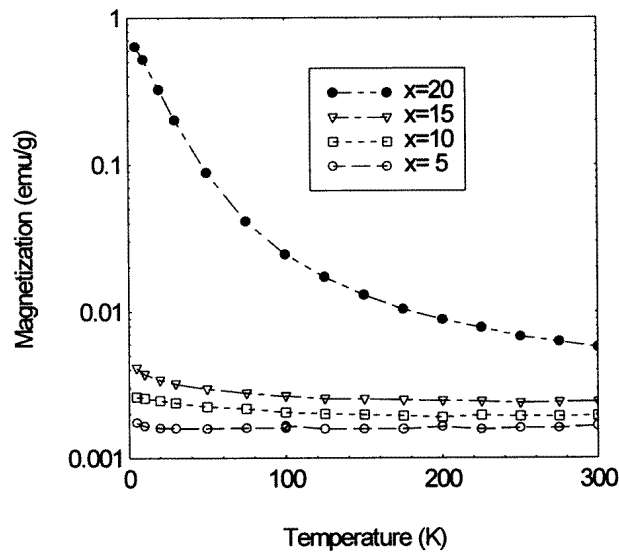
where  $N_{1,ij}$  is equal to the nearest-neighbour number of  $j$ -atoms in the first shell of an  $i$ -atom. Under the assumptions that there is no chemical preference of certain types of atom in the first coordination shell of a given atom, i.e.  $N_{1,ij} = c_j N$  and that the distances  $r_{1,ij}$  are equal to the atomic diameter for  $i = j$  and equal to the nearest-neighbour distances in the corresponding intermetallic alloys for  $i \neq j$ , the first maximum in  $G(r)$  was calculated as a superposition of Gaussian curves,  $g_{ij}(r) = \exp[-a(r - r_{1,ij})^2]$ .

Figure 3 compares the measured and calculated values. The shape of the first maximum in  $G(r)$  can be reproduced by the calculation explained above. The position and shape of the maximum and the dependence on the iron content are in agreement. The mean value  $r_1$  is shifted without change of the partial distances  $r_{1,ij}$ . The reduction of the weights  $w_{\text{ZrZr}}$  from 0.56 for  $x = 0$  to 0.39 for  $x = 20$ , and the enhancement of  $w_{\text{FeZr}}$  from 0.0 for  $x = 0$  to 0.20 for  $x = 20$  lead to the increasing asymmetry of the maximum. The observed differences of the first peak of  $G(r)$  can, therefore, be explained assuming randomly distributed iron atoms.

The measurement of the magnetization as a function of the applied field showed neither any remanent magnetization nor a magnetic hysteresis in the investigated composition range of the samples. Thus, ferromagnetism and spin glass behaviour can be excluded, and only positive fields are discussed further. Figure 4 shows the temperature dependence of the



**Figure 3.** First maximum of the atomic pair correlation function (symbols, experimental data; dashed lines, calculated values).



**Figure 4.** Magnetization of amorphous  $(\text{Zr}_{65}\text{Al}_{7.5}\text{Cu}_{17.5}\text{Ni}_{10})_{100-x}\text{Fe}_x$  at  $\mu_0 H = 0.1$  T for different temperatures.

magnetization at 0.1 T. The magnetization is low and nearly constant for  $x = 5$ . The susceptibility is about  $2 \times 10^{-6} \text{ cm}^3 \text{ g}^{-1}$ . We interpret this behaviour as the temperature independent Pauli paramagnetism of the conduction electrons. With increasing  $x$  an increase of the magnetization is observed. The low temperature magnetization becomes more nonlinear. The magnetization of the  $x = 20$  alloy differs significantly from that of the

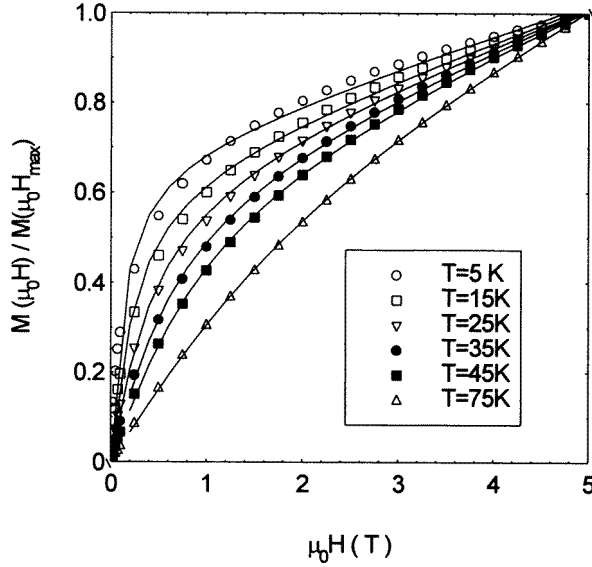


**Figure 5.** Temperature and field dependence of the magnetization of  $(\text{Zr}_{65}\text{Al}_{17.5}\text{Cu}_{17.5}\text{Ni}_{10})_{100-x}\text{Fe}_x$ ;  $\mu_0 H_{max} = 5$  T.

samples with  $x \leq 20$  both with respect to the magnitude and the temperature dependence and is discussed in more detail.

Figure 5 shows the magnetization as a function of the magnetic field for  $x = 20$  and the temperature as parameter. The magnetization fits well to

$$M(H)/M(H_{max}) = \chi_{para}^0 H + a_0 \int_{1/\mu_B}^{\mu_{max}} L\left(\frac{\mu H}{k_B T}\right) d\mu \quad (3)$$

where  $L(y) = \coth y - 1/y$  is the Langevin function,  $\chi_{para} = \chi_{para}^0 M(H_{max})$  is the paramagnetic susceptibility and  $H_{max} = 5$  T. The second term in (3) describes the field and temperature dependence of a set of magnetic clusters. The magnetic moments of the clusters are assumed to be equally distributed between  $1 \mu_B$  and  $\mu_{max}$  and no interaction between the clusters is presumed. In table 2, the mean magnitude moment of the clusters,  $\langle \mu \rangle = 0.5 \mu_{max}$ , and its temperature dependence is given. Except for  $T = 5$  K, the mean moment decreases continuously with increasing temperature. The estimates for the other parameters in expression (3) are  $a_0 = 0.7$  and  $\chi_{para}^0 = 7-8 \times 10^{-6}$ . Taking into account the mass density  $g \cong 6.8 \text{ g cm}^{-3}$  of the sample the density of moments  $N_\mu^0$  (respectively clusters) is then given by

$$N_\mu^0 \cong a_0 M(H_{max}) / (\mu_{max}/2) \cong 6.4-7.0 \times 10^{17} / g \cong 4.3-4.8 \times 10^{18} \text{ cm}^{-3}.$$

The magnetic results for the alloy with  $x = 20$  suggest that there is a ferromagnetic coupling of the Fe atoms within a given cluster whereas the interaction between the clusters is negligible. The ferromagnetic clusters are very small. Assuming a mean moment of  $1-2 \mu_B$  per magnetic Fe atom one cluster consists, on average, of about  $10^2$  atoms. Multiplying the mean cluster size by  $N_\mu^0$ , the fraction of Fe atoms situated in magnetic clusters is estimated to be about 0.05% of all iron atoms. This corresponds to a volume fraction of iron clusters of less than 0.01%.

**Table 2.** Magnetic properties of amorphous  $(\text{Zr}_{65}\text{Al}_{7.5}\text{Cu}_{17.5}\text{Ni}_{10})_{80}\text{Fe}_{20}$ .  $H_{max} = 5$  T,  $1$  emu  $= 1.08 \times 10^{20} \mu_B$ .

$T$ (K)	$\langle \mu \rangle = 0.5\mu_{max}$ ( $\mu_B$ )	$M(H_{max})$ (emu $\text{g}^{-1}$ )	$N_{\mu}^0$ ( $10^{20} \text{g}^{-1}$ )
5	113	1.88	0.0126
15	183	1.70	0.0070
25	171	1.54	0.0068
35	156	1.39	0.0067
45	141	1.26	0.0068
75	110	0.93	0.0064

In the temperature range below 75 K, the local moments in amorphous binary Fe–Zr alloys vanish for an iron content of  $C_{Fe} \leq 28$  at.% whereas the alloys become ferromagnetic for  $28 \text{ at.\%} < C_{Fe} < 90 \text{ at.\%}$  [1, 10]. For the present alloy with  $x = 20$ , we determined local moments of ferromagnetic clusters but no macroscopic ferromagnetism, even at temperatures as low as 5 K. As discussed in [10] the local moments in amorphous Fe–Zr alloys increase with the reduction of the hybridization of the Fe 3d and Zr 4d orbitals at increasing iron concentration. This should be also the case if the concentration of other late 3d transition metals such as Ni and Cu is increased. In the alloy with  $x = 20$  we have a total 3d transition metal concentration of  $C_{3dTM} = 42$  at.% which is well above the threshold determined in [10] for the occurrence of local magnetic moments at 75 K. On the other hand, Ni and Cu have more completely filled 3d shells than iron. Therefore, they have low or vanishing local moments. As a consequence for the present samples, ferromagnetism is only expected in regions where the local iron concentration exceeds a certain limit.

Now we estimate the probability of finding clusters of Fe atoms of a certain minimum size under the supposition confirmed experimentally that the Fe atoms are distributed at random in the amorphous alloy. The distribution of the Fe atoms in the alloy is simulated by an interaction-free random set—the Boolean model [11]. The regions occupied by Fe atoms are characterized by the size distribution

$$f(l) = \lambda \exp(-\lambda l) \quad \lambda = (1.24/D_{Fe}) \ln(1/c_{Fe}) \quad (4)$$

where  $l$  is the length of a random line through an arbitrary Fe cluster (chord length),  $1/\lambda$  is the mean chord length,  $D_{Fe}$  is the diameter of Fe atoms and  $c_{Fe}$  is the volume fraction of the regions containing the Fe atoms. The volume fraction,  $v$ , of Fe clusters of size  $l \geq l_c$  is

$$v = c_{Fe} \int_{l_c}^{\infty} l \lambda^2 \exp(-\lambda/l) dl = c_{Fe} (1 + n_c z) \exp(-n_c z) \quad (5)$$

where  $z = 1.24 \ln(1/c_{Fe})$ , and  $n_c$  is the cluster size measured in  $D_{Fe}$ . Taking into account the mass density of the samples, the atomic radii and atomic weights of the constituents and assuming a dense random packing structure with a packing fraction of 0.63 for the Fe clusters, the size distribution (5) of the Fe clusters can be transformed in a distribution giving the fraction of Fe atoms situated in clusters with at least  $n_c$  atoms. This distribution is shown in figure 6 for  $x = 5$ –20. For the sample with  $x = 20$ , 0.05 at.% of all Fe atoms are distributed in pure Fe clusters containing more than about 120 atoms. (It should be noted that this estimate is based on the assumption that the Fe atoms are distributed at random without any attractive or repulsive interaction.) This corresponds well with the interpretation of the magnetic measurements for the sample with 20 at.% Fe. Figure 6 shows also that the fraction of Fe atoms situated in pure Fe clusters with more than about 100 atoms decreases dramatically if the Fe content is reduced to  $x \leq 15$ . This is also in agreement with

the experimental results. Furthermore, the comparison of the volume fraction of magnetic clusters estimated by the magnetization experiments and the one calculated from the random model shows that Fe clusters containing less than about 100 atoms do not have magnetic moments. So we can draw the following conclusions.

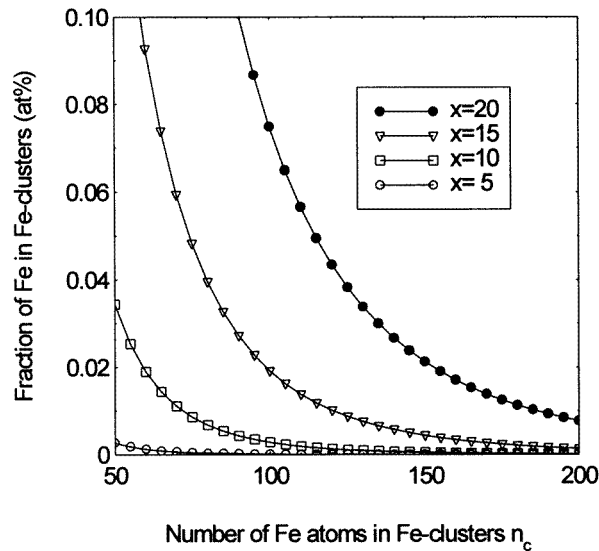


**Figure 6.** The fraction of iron atoms situated in iron clusters containing at least  $n_c$  iron atoms against  $n_c$  (theoretical results calculated for the model with randomly distributed iron atoms).

The Fe atoms in amorphous  $(\text{Zr}_{65}\text{Al}_{7.5}\text{Cu}_{17.5}\text{Ni}_{10})_{100-x}\text{Fe}_x$  alloys ( $5 \leq x \leq 20$ ) are distributed at random. There is no decomposition due to attractive interaction between the Fe atoms. The existing clusters of Fe atoms are solely generated by random fluctuations. For 20 at.% Fe content, about 0.05% of all Fe atoms are situated in Fe clusters with minimum size of about 120 atoms. A cluster of this type creates a local magnetic moment. There is a broad distribution of the moments and the mean value is of the order of  $10^2 \mu_B$  at temperatures  $T \leq 75$  K. Fe clusters with a size below about 100 atoms do not show any local magnetic moment.

## References

- [1] Zhang T, Inoue A and Masumoto T 1991 *Mater. Trans. JIM* **32** 1005
- [2] Inoue A, Zhang T and Masumoto T 1993 *J. Non-Cryst. Solids* **156–158** 473
- [3] Peker A and Johnson W L 1993 *Appl. Phys. Lett.* **63** 2342
- [4] Inoue A, Zhang T, Itoi T and Takeuchi A 1997 *Mater. Trans. JIM* **38** 359
- [5] Inoue A, Koshiba H, Zhang T and Makino A 1997 *Mater. Trans. JIM* **38** 577
- [6] Eckert J, Matern N, Seidel M and Schultz L 1997 *Mater. Res. Soc. Symp. Proc.* vol 455 (Pittsburgh, PA: Materials Research Society) p 465
- [7] Cargill G S 1975 *Solid State Physics* vol 30 (New York: Academic) p 227
- [8] Klug H P and Alexander L E 1959 *X-Ray Diffraction Procedures for Polycrystalline and Amorphous Materials* (New York: Wiley)
- [9] Wagner C N J 1972 *Liquid Metals, Chemistry and Physics* ed S Z Beer (New York: Dekker) p 257
- [10] Yu M Y and Kakehashi Y 1996 *J. Magn. Magn. Mater.* **162** 189
- [11] Stoyan D, Kendall W S and Mecke J 1995 *Stochastic Geometry and its Applications* 2nd edn (Chichester: Wiley)